

Theoretical Analysis of Electronic and Magnetic Properties of NaV_2O_4 : Crucial Role of the Orbital Degrees of Freedom

Z. V. Pchelkina,^{1,2,*} I. V. Solovyev,^{3,†} and R. Arita^{4,5}

¹*Institute of Metal Physics, Russian Academy of
Sciences-Ural Division, 620990 Ekaterinburg, Russia*

²*Theoretical Physics and Applied Mathematics Department,
Ural Federal University, Mira Str. 19, 620002 Ekaterinburg, Russia*

³*Computational Materials Science Unit,
National Institute for Materials Science,
1-2-1 Sengen, Tsukuba, Ibaraki 305-0047, Japan*

⁴*Department of Applied Physics, Graduate School of Engineering,
The University of Tokyo, 7-3-1 Hongo,
Bunkyo-ku, Tokyo 113-8656, Japan*

⁵*PREST, Japan Science and Technology Agency,
4-1-8 Honcho, Kawaguchi, Saitama 332-0012, Japan*

(Dated: January 2, 2019)

Abstract

Using realistic low-energy model with parameters derived from the first-principles electronic structure calculation, we address the origin of the quasi-one-dimensional behavior in orthorhombic NaV_2O_4 , consisting of the double chains of edge-sharing VO_6 octahedra. We argue that the geometrical aspect alone does not explain the experimentally observed anisotropy of electronic and magnetic properties of NaV_2O_4 . Instead, we attribute the unique behavior of NaV_2O_4 to one particular type of the orbital ordering, which respects the orthorhombic $Pnma$ symmetry. This orbital ordering acts to divide all t_{2g} states into two types: the ‘localized’ ones, which are antisymmetric with respect to the mirror reflection $y \rightarrow -y$, and the symmetric ‘delocalized’ ones. Thus, NaV_2O_4 can be classified as the double exchange system. The directional orientation of symmetric orbitals, which form the metallic band, appears to be sufficient to explain both quasi-one-dimensional character of interatomic magnetic interactions and the anisotropy of electrical resistivity.

PACS numbers: 71.20.-b, 71.70.Gm, 75.30.Et

I. INTRODUCTION

Double exchange (DE) is the key concept in the physics of strongly correlated systems, characterizing the properties of itinerant electrons, traveling in the lattice of localized (atomic) spins.¹

The situation becomes increasingly interesting when there are several degenerate orbitals, which become involved into the DE processes. Typically, each orbital is highly nonspherical and can assist the electron transfer only in some spacial directions, which can differ substantially, depending on the shape of the occupied orbital. Thus, the itinerant electron can “choose” the orbital where to reside and, depending on it, choose a path for its traveling in the solid. Of course, the transport properties will crucially depend on such a choice. Moreover, each guess for the orbital configuration has a feedback effect and involves some elements of the self-organization, typically through developing certain magnetic texture, which tends to stabilize the assumed orbital configuration, at least locally. Alternatively, each change of the magnetic state leads to the orbital-selective reconstruction of the electronic structure, which can be sufficient to stabilize the magnetic state.² All these phenomena are largely involved in the physics of pseudocubic perovskite manganites and predetermine the rich variety of their electronic and magnetic properties.³

In this paper we propose that the DE physics can lead to a number of interesting effects when it brought in contact with the unusual crystal structure of recently synthesized mixed-valence ($d^{1.5}$) NaV_2O_4 compound consisting of double chains of edge-sharing VO_6 octahedra (see Fig. 1).^{4,5}

The properties of NaV_2O_4 are indeed very intriguing. It has orthorhombic space group $Pnma$, where there are four formula units in the primitive cell, and two nonequivalent vanadium types V1 and V2, which are numbered as 1-4 and 5-8, respectively (Fig. 1).⁵ The vanadium atoms are surrounded by slightly distorted edge-sharing octahedra which form the zig-zag chains propagating in the b -direction.

The single-crystalline NaV_2O_4 remains metallic down to 40mK. Nevertheless, the low-temperature properties of NaV_2O_4 are characterized by the strong anisotropy of the electrical resistivity: $\rho_{\perp}/\rho_{\parallel} > 20$, where the symbols \parallel and \perp stand for the directions being parallel and perpendicular to the crystallographic b -axis, respectively. In this sense, NaV_2O_4 is regarded as the quasi-one-dimensional (quasi-1D) compound.

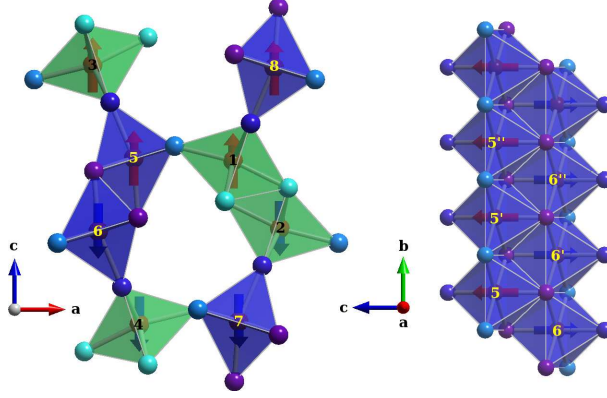


FIG. 1: (color online). The schematic view on the crystal structure and the AFM arrangement of eight vanadium atoms in the primitive cell of NaV_2O_4 . Eight vanadium atoms in the primitive cell are in the centers of octahedra and denoted by numbers (1-4 correspond to the type V1 and 5-8 – to the type V2). Small spheres in the corners of octahedra stand for the nonequivalent oxygen atoms. Na atoms are hidden for clarity.

The magnetic susceptibility (χ) of NaV_2O_4 has a peak at around $T_N=140$ K, indicating an antiferromagnetic (AFM) transition. On the other hand, the fitting of χ in terms of the Curie-Weiss law well above T_N yields positive Weiss constant, indicating at the predominantly ferromagnetic (FM) character of interactions.⁴ Furthermore, the anisotropy of electrical resistivity rapidly deteriorates above T_N .^{4,5} These results, together with the metallic character of conductivity along the b -axis gave rise to a hypothesis that within each zig-zag double-chain, the intrachain interaction should be FM while the interchain interaction is AFM (Fig. 1).⁴ Thus, it seems that not only the electrical resistivity, but also the magnetic structure of NaV_2O_4 is highly anisotropic and these two anisotropies are coupled to each other.

Later on, several attempts to clarify the magnetic structure of NaV_2O_4 have been undertaken in the experiments on the neutron scattering,⁶ the muon-spin rotation,⁷ and the nuclear magnetic resonance (NMR).⁸ Nevertheless, the magnetic structure remains a matter of controversy. For example, earlier neutron-scattering measurements have been interpreted in terms of the incommensurate spin-density wave order with $\mathbf{q} = (0, 0.191, 0)$, in units of $2\pi/b$.⁶ However, more recent muon-spin rotation studies favor the helical magnetic structure, where the magnetic moments lie in the ac plane and propagate along the b axis. This means

that some of the intrachain interactions should be AFM, which confronts the hypothesis based on the magnetization measurements.⁴ Finally, there are also experimental proposals that NaV_2O_4 may exhibit several consequent AFM transitions below T_N .^{7,8,10}

The purpose of this work is to build some theoretical background for understanding these electronic and magnetic properties of NaV_2O_4 . First, we construct a realistic low-energy model (Sec. II), which aims to describe the electronic and magnetic properties of NaV_2O_4 . Then, we analyze this model in the mean-field Hartree-Fock (HF) approximation (Sec. III). Although HF is a crude approximation for metallic systems, we will be able to argue, on a semi-quantitative level, that the main details of the electronic and magnetic structure are well anticipated from such a model analysis and can be attributed to the particular type of the orbital ordering in the metallic state. Once the orbital ordering is established, NaV_2O_4 has many things in common with the DE systems. Finally, a brief summary will be given in Sec. IV.

II. METHOD

In our theoretical analysis, we follow the strategy, which was developed in the previous publications and which can be called as “realistic modeling of strongly correlated systems” (see Ref. 11 for a review). First, we calculate the electronic structure of NaV_2O_4 in the local-density-approximation (LDA), using the experimental parameters of the crystal structure, measured at $T=300$ K.^{5,12} The obtained electronic structure is in a good agreement with the previous calculations.⁴ Then, we construct the low-energy Hubbard-type model for the t_{2g} bands of NaV_2O_4 , located near the Fermi level, and derive all parameters of such model from the first-principles electronic structure calculations. The details of the computational procedure can be found in Ref. 11. In a number of cases, we have also constructed and solved the five-orbital model, which describes the behavior of both t_{2g} and e_g bands of NaV_2O_4 .

The model includes three sets of parameters: the crystal field (CF), transfer integrals, and screened Coulomb interactions.

The splitting of three t_{2g} levels by the CF has the following structure (in meV): (0, 46, 204) and (0, 10, 264), at the inequivalent vanadium types V1 and V2, respectively. Two lowest levels are nearly degenerate and not disrupted by the crystal distortion. This type of the CF splitting is favored by the DE interactions and minimizes the kinetic energy of electrons.

Nevertheless, two lower t_{2g} orbitals can still mix with the upper one by the transfer integrals. This mixing can be relatively strong.

The behavior of some transfer integrals is explained in Fig. 2, in the local coordinate frame, which diagonalizes the CF Hamiltonian. The largest transfer integrals operate between nearest-neighbor (NN) V-atoms in the chains 1-1' (3-3') and 5-5' (8-8'). The transfer integrals between the chains are somewhat weaker, but still comparable with the ones within the chains. Thus, the structure of transfer integrals in is essentially three-dimensional, and alone does not explain the quasi-1D character of the electronic and magnetic properties of NaV_2O_4 .

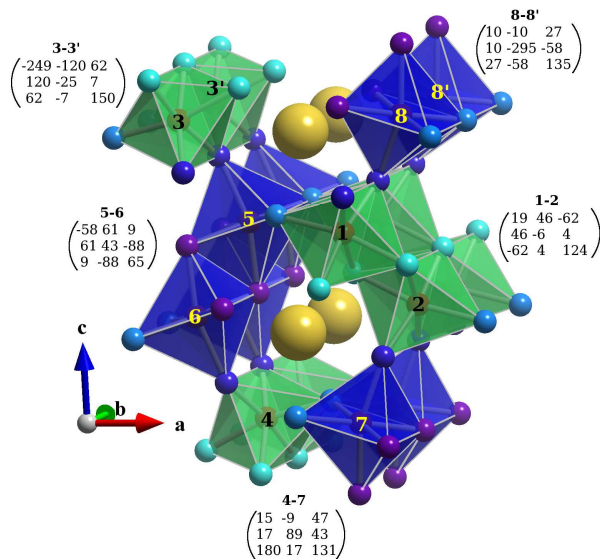


FIG. 2: (color online). Fragment of the crystal structure of NaV_2O_4 with the matrices of transfer integrals between nearest neighbors. Each matrix is computed in the crystal field coordination frame, in the basis of t_{2g} states. The matrix elements are measured in meV. The big yellow spheres stand for Na atoms. Other notations are the same as in Fig. 1.

The screened Coulomb interactions in the t_{2g} -band can be computed in two steps,¹¹ by applying the constrained LDA and the random-phase approximation (RPA) for the screening. Roughly speaking, the first technique takes into account the screening of atomic orbitals, while the second one – the self-screening by the same $3d$ -electrons, which participate in the formation of other bands due to the hybridization effects. The fitting of screened interactions in terms of two Kanamori parameters yields the following characteristic values of the

intra-orbital Coulomb interaction $\mathcal{U}= 3.15$ (3.19) eV and the intraatomic exchange coupling $\mathcal{J}= 0.63$ (0.63) eV, for the vanadium type V1 (V2).¹³

All parameters of the model Hamiltonian can be found in Ref. 14. After the construction, the model is solved in the HF approximation.¹¹ Since the HF approximation is known to have limitations for the metallic systems, we will also discuss possible impact of correlation interactions on the semi-quantitative level.

Before going into details, we would like to emphasize that the analysis of electronic and magnetic properties of NaV_2O_4 can be greatly simplified by considering the symmetry aspects. It appears that besides the CF splitting, which lifts the degeneracy of atomic t_{2g} -levels and thus specifies subspace of the occupied orbitals, another important factor is the *symmetry* of orbitals, which are obtained from the diagonalization of the CF Hamiltonian at each V-site i . They can be schematically denoted as $(\phi_{S1}^i, \phi_A^i, \phi_{S2}^i)$, for the vanadium type V1 ($i= 1-4$), and $(\phi_A^i, \phi_{S1}^i, \phi_{S2}^i)$, for the vanadium type V2 ($i= 5-8$). In the other words, these are the eigenvectors of the CF Hamiltonian, which corresponds to the eigenvalues (the CF splitting), listed above. In these notations, ϕ_S^i and ϕ_A^i are symmetric and antisymmetric eigenvectors with respect to the mirror reflection $y \rightarrow -y$, which transform each V-site to itself (with the additional shift by $\mathbf{b}/2$). For example, for the inequivalent V-sites 1 and 5 (see Fig. 1), these orbitals have the following form: $\phi_{S1}^1 = 0.84|3z^2-r^2\rangle + 0.19|zx\rangle + 0.51|x^2-y^2\rangle$, $\phi_A^1 = 0.94|xy\rangle - 0.33|yz\rangle$, $\phi_{S2}^1 = 0.42|3z^2-r^2\rangle - 0.82|zx\rangle - 0.38|x^2-y^2\rangle$, $\phi_A^5 = 0.27|xy\rangle - 0.96|yz\rangle$, $\phi_{S1}^5 = 0.01|3z^2-r^2\rangle + 0.16|zx\rangle + 0.99|x^2-y^2\rangle$, and $\phi_{S2}^5 = 0.41|3z^2-r^2\rangle + 0.90|zx\rangle - 0.15|x^2-y^2\rangle$. The shape of these orbitals is explained in Fig. 3. Similar orbitals at other V-sites can be generated by applying the symmetry operations of the space group $Pnma$. The fact that two lowest levels, which are split off by the crystal field, belong to different representations (correspondingly, symmetric and antisymmetric one) has very important consequences and greatly reduces the number of possible solutions of the electronic model, which we have to consider. Indeed, due to the large orbital polarization, which is driven by the on-site Coulomb interaction \mathcal{U} , the local populations of occupied orbitals (n), corresponding to the $d^{1.5}$ configuration of V-sites, can be either 1 or 1/2. Since these orbitals belong to different representations and, therefore, do not mix with each other, we have to consider only four possible HF solutions, corresponding to the following populations of the symmetric and antisymmetric orbitals of the vanadium types V1 and V2: $(n_S^{V1}, n_A^{V1}, n_S^{V2}, n_A^{V2}) = (1/2, 1, 1/2, 1)$, $(1, 1/2, 1/2, 1)$, $(1/2, 1, 1, 1/2)$, and $(1, 1/2, 1, 1/2)$. Moreover, the antisymmetric orbitals at

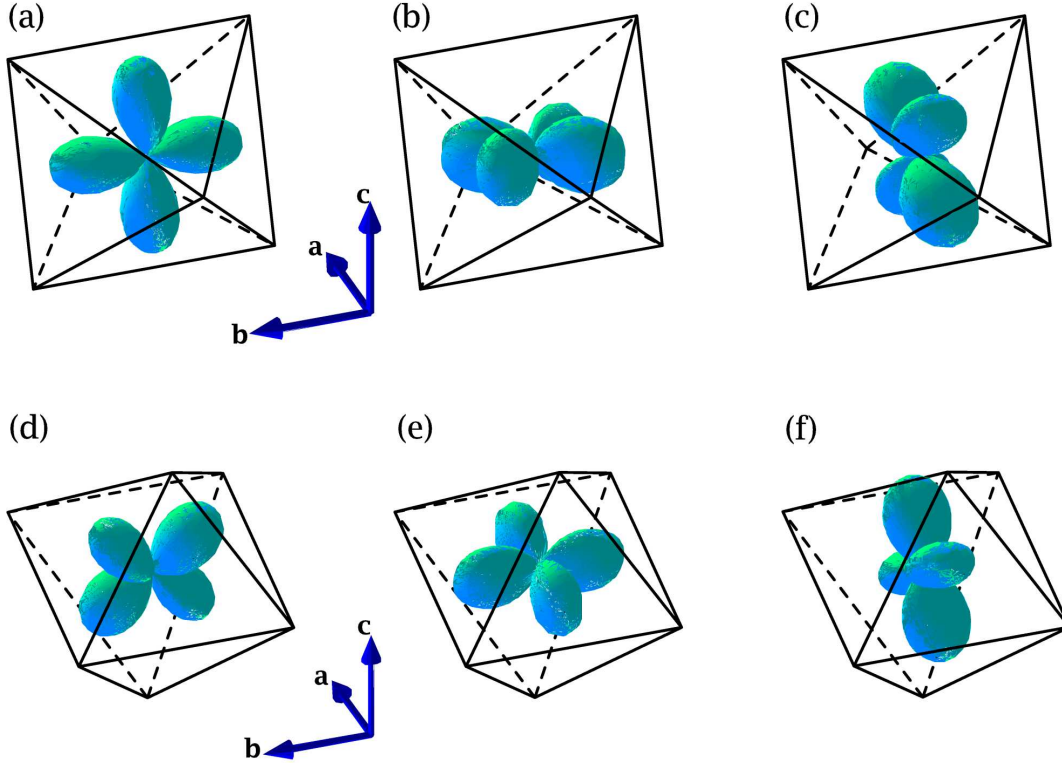


FIG. 3: (color online). Electron density distribution, corresponding to the crystal-field orbitals ϕ_{S1}^1 (a), ϕ_A^1 (b), and ϕ_{S2}^1 (c) at the V-site 1; and ϕ_A^5 (d), ϕ_{S1}^5 (e), and ϕ_{S2}^5 (f) at the V-site 5.

each site will simply coincide with ϕ_A^i (the only possible antisymmetric orbitals in the t_{2g} basis), while each occupied symmetric orbital is a linear combination of ϕ_{S1}^i and ϕ_{S2}^i , which is obtained in the process of iterative solution of the HF equations. Finally, for each orbital configuration, we should find the magnetic solution, corresponding to the total energy minimum.

The behavior of NN transfer integrals in the chains can be also understood, by considering the symmetry arguments. Since for the edge-sharing geometry of the VO_6 octahedra, the main contribution to the NN integrals is caused by the $dd\sigma$ interactions, which are possible only between orbitals of the $|3z^2-r^2\rangle$ and $|x^2-y^2\rangle$ type, it is reasonable to expect that the transfer integrals in the bonds 1-1' (3-3') and 5-5' (8-8') will be large between symmetric orbitals, which have these components, and small – between antisymmetric ones, which do not have them due to the symmetry constraint. This is indeed roughly consistent with the behavior of the transfer integrals, depicted in Fig. 2. Thus, from the viewpoint of the

DE interactions in the chains, it is more favorable energetically to make the antisymmetric orbitals fully localized ($n=1$), and to construct the metallic band from the symmetric orbitals ($n=1/2$). This constitutes the main idea behind results of calculations, which will be presented in the next section.

III. RESULTS AND DISCUSSIONS

We start with the analysis of the FM spin ordering, and attempt to stabilize different orbital structures in the HF approximation, as described above. By doing so, we were able to obtain only two orbital configurations, corresponding to $(n_S^{V1}, n_A^{V1}, n_S^{V2}, n_A^{V2}) = (1/2, 1, 1/2, 1)$ and $(1, 1/2, 1/2, 1)$. In the following, we will call them as $\mathcal{O}1$ and $\mathcal{O}2$, respectively. Two other solutions systematically converge to one of these two. The $\mathcal{O}1$ configuration appears to be lower in energy by about 9 meV per one formula unit – the reason will become clear below. The behavior of one-electron densities of states, corresponding to the orbital configurations $\mathcal{O}1$ and $\mathcal{O}2$, is explained in Fig. 4. Both solutions are half-metallic (HM). As expected for the $\mathcal{O}1$ configuration, the majority (\uparrow)-spin A -states are almost fully occupied (the small weight in the unoccupied part of the spectrum is due to the mixing between states of the A - and S -symmetry, which is caused by transfer integrals – see Fig. 2). The metallic band is mainly formed by the $S1$ -states, with the small admixture of the $S2$ -states. For the $\mathcal{O}2$ configuration, two V-sites display different behavior: at the site V1, the \uparrow -spin bands of the A and S -symmetry are half- and totally-filled, respectively, while at the site V2, this filling is reversed. Moreover, the $\mathcal{O}2$ alignment leads to a pseudo-gap at the Fermi level.

The parameters of interatomic magnetic interactions are listed in Table I. They were calculated for two orbital configurations, by applying the perturbation theory expansion with respect to the infinitesimal spin rotations near the FM state.¹⁵ This procedure corresponds to the *local* mapping of the total energy change near each equilibrium onto the spin model $\hat{\mathcal{H}}_S = -\sum_{i>j} J_{ij} \mathbf{e}_i \mathbf{e}_j$, where \mathbf{e}_i is the *direction* of magnetic moment at the site i . The advantage of this procedure is that the parameters J_{ij} depend on the electronic structure of the spin-orbital state, in which they are calculated, and can be regarded as the local probe of this state. One can clearly see that the change of the orbital state $\mathcal{O}1 \rightarrow \mathcal{O}2$ has a dramatic effect on magnetic interactions in the V1 chains and results in the sharp drop of the $J_{11'}$ interaction. Instead, the interchain interaction J_{18} tends to increase due to the

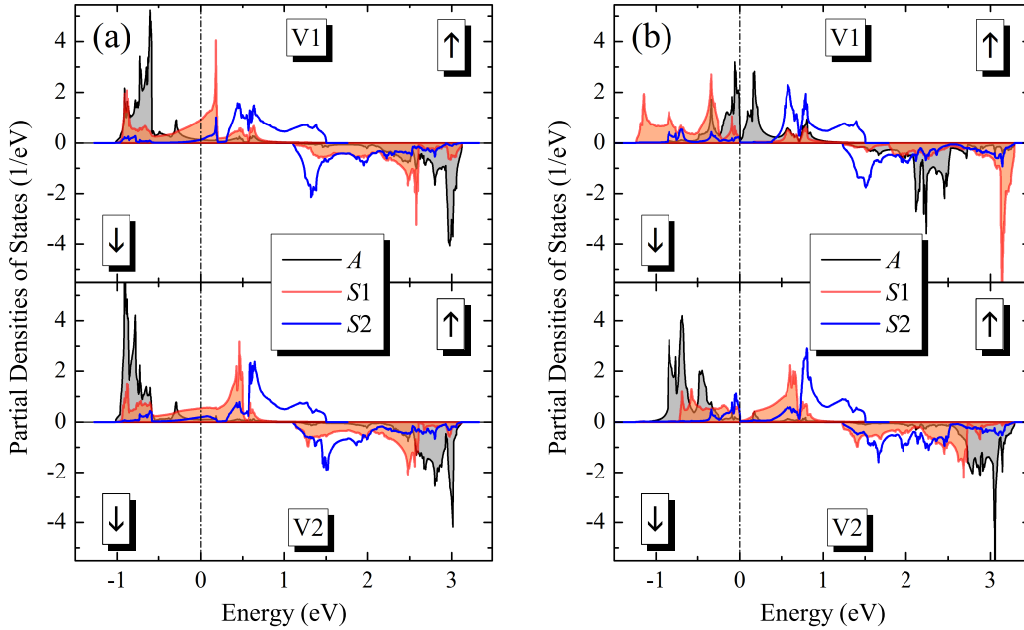


FIG. 4: (color online). Partial densities of states, corresponding to the ferromagnetic spin ordering with different orbital configurations: $\mathcal{O}1$ (a) and $\mathcal{O}2$ (b). V1 and V2 denote two inequivalent vanadium sites, and A, S1 and S2 – contributions of one antisymmetric and two symmetric orbitals, obtained from the diagonalization of the crystal field. The Fermi level is at zero energy (shown by dashed-dotted line).

orbital reconstruction. On the other hand, the orbital configuration of V2 does not change so much. Therefore, two solutions yield similar values of interatomic magnetic interactions $J_{55'}$ and J_{56} . As a test, we have also constructed the five-orbital model ($t_{2g}+e_g$) and performed similar calculations of interatomic magnetic interactions. For $\mathcal{O}1$, these results are also shown in Table I. One can see that three- and five-orbital models provide similar values of J_{ij} . Thus, we have confirmed that the three-orbital model captures basic magnetic properties of NaV_2O_4 pretty well, and in the following we will focus on the analysis of only this model. We have also confirmed that the change of the spin ordering for a given orbital ordering does not significantly modify the behavior of interatomic magnetic interactions. Therefore, in the following we will focus on the behavior of parameters obtained in the FM state.

Let us concentrate on the low-energy configuration $\mathcal{O}1$ and discuss the origin of the AFM instabilities, which were observed in the experiment. From the analysis of J_{ij} (Table I), one

TABLE I: Main parameters of interatomic magnetic interactions (in meV), calculated near the ferromagnetic state for two orbital configurations $\mathcal{O}1$ and $\mathcal{O}2$. Most of the calculations have been performed for the three-orbital model (the so-called ‘ t_{2g} model’). In addition, some test calculations for the $\mathcal{O}1$ configuration have been also performed using the five-orbital model (the so-called ‘ $t_{2g}+e_g$ model’).

bond	$\mathcal{O}1$ ($t_{2g}+e_g$)	$\mathcal{O}1$ (t_{2g})	$\mathcal{O}2$ (t_{2g})
1-1'	35.9	30.1	0.5
1-2	2.9	2.0	0.4
1-5	9.3	7.7	7.1
1-8	9.6	10.8	15.4
1-1''	-5.8	-5.4	-0.6
5-5'	37.8	30.0	26.0
5-6	4.1	3.8	4.1
5-5''	-3.2	-1.0	0.4

can see that all NN interactions are FM. Furthermore, the FM coupling within the chains ($J_{11'}$ and $J_{55'}$) is the strongest one, while the coupling between the chains of equivalent V-atoms (J_{12} and J_{56}), is considerably weaker (and weaker than the interactions 1-5 and 1-8 between different double chains).

Thus, the most probable candidate for the AFM ground state should be the one, where the spins between the chains of equivalent vanadium atoms are coupled antiferromagnetically and the double-chains themselves are coupled ferromagnetically (i.e., corresponding to the $\uparrow\downarrow\uparrow\downarrow\uparrow\downarrow\uparrow$ spin alignment at the V-atoms 1-8, depicted in Fig. 1), which seems to consistent with the experimental suggestion.⁴ In this sense, it is right to say that the quasi-one-dimensional magnetic structure, realized in NaV_2O_4 , is due to the $\mathcal{O}1$ orbital ordering. Moreover, the second-neighbor interactions in the chains ($J_{11''}$ and $J_{55''}$) are AFM. Such a behavior can be viewed as a precursor of the helical order, which was suggested in some experimental studies.⁸ Note that the AFM character of the second-neighbor interactions is expected for the DE systems.¹⁶ Nevertheless, our calculations seem to overestimate the tendency towards the ferromagnetism. For example, the FM character of interactions J_{12} and J_{56} (Table I) definitely favors the FM ground state, rather than the the AFM $\uparrow\downarrow\uparrow\downarrow\uparrow\downarrow\uparrow$ one.

TABLE II: Results of decomposition of nearest-neighbor magnetic interactions for the orbital configuration $\mathcal{O}1$ in terms of double exchange (J_{ij}^{DE}) and superexchange (J_{ij}^{SE}). All values are in meV. The parameter of intraatomic exchange splitting Δ_{ex} was set equal to 2.8 eV in order to satisfy the condition $J_{ij} = J_{ij}^{\text{DE}} + J_{ij}^{\text{SE}}$ for the largest exchange coupling J_{18} between different V-types. For other bonds, this condition is satisfied only approximately.

bond	J_{ij}^{DE}	J_{ij}^{SE}
1-1'	45.5	-18.8
1-2	4.2	-2.4
1-5	17.4	-9.5
1-8	21.6	-10.9
5-5'	44.4	-17.4
5-6	9.1	-5.7

The same tendency was found in the total energy calculations, where the AFM solution was systematically higher than the FM one ($\Delta E = 9$ and 11 meV per one formula unit in the three- and five-orbital model, respectively). Moreover, since FM $J_{11'}$ ($J_{55'}$) largely exceeds the AFM $J_{11''}$ ($J_{55''}$), the helical ordering cannot be realized either.

We attribute these discrepancies to the HF approximation, which has some limitations for metallic systems. Below, we qualitatively discuss the role of correlation interactions, beyond the HF approximation, and argue that they can indeed resolve the problem. For these purposes, it is convenient to decompose each NN interaction in terms of double exchange and superexchange (SE) contributions: $J_{ij} = J_{ij}^{\text{DE}} + J_{ij}^{\text{SE}}$. Formally, such a decomposition can be done for the HM electronic structure, by assuming that the splitting between the majority (\uparrow)- and minority (\downarrow)-spin states can be described by a single parameter Δ_{ex} and expanding each J_{ij} in terms of $1/\Delta_{\text{ex}}$. Thus, Δ_{ex} has a meaning of (averaged) intraatomic spin splitting. Then, the zeroth-order term in this expansion corresponds to J_{ij}^{DE} , while the first-order term – to J_{ij}^{SE} . The details can be found in Ref. 17. The parameters of such an expansion are listed in Table II. We treat Δ_{ex} as an adjustable parameter. Then, by choosing $\Delta_{\text{ex}} \approx 2.8$ eV, the values of interatomic magnetic interactions J_{ij} in Table I can be approximated reasonably well by the combination $J_{ij} \approx J_{ij}^{\text{DE}} + J_{ij}^{\text{SE}}$ of DE and SE interactions, listed in Table II. Of course, the agreement is not perfect, mainly because the

decomposition relies on the rigid energy splitting between the \uparrow - and \downarrow -spin states, which is an approximation. Nevertheless, $\Delta_{\text{ex}} \approx 2.8$ eV seems to be a good choice for the averaged splitting in the HF approximation (see Fig. 4). As expected, all DE interactions are FM, while SE interactions are AFM. The large FM coupling within the chains is stabilized by the $\mathcal{O}1$ orbital ordering, which maximizes the DE interactions (for comparison, the $\mathcal{O}2$ orbital arrangement yields $J_{11'}^{\text{DE}} = 25.5$ meV and $J_{11'}^{\text{SE}} = -26.5$ meV).

Then, it is reasonable to expect that Δ_{ex} will be screened by correlation interactions. For example, such an effect is well known in the theory of the homogeneous electron gas.¹⁸ Similar tendency was found in the total energy calculations for the low-energy model, which was constructed for the series of HM systems: the correlation interactions, treated in RPA, systematically decrease the effective intraatomic spin splitting and, in a number of cases, make this HM state unstable.¹⁹ Thus, it is clear that the reduction of Δ_{ex} , caused by the metallic screening effects, will strengthen J_{ij}^{SE} , which is proportional to $1/\Delta_{\text{ex}}$, and shift the balance of magnetic interactions towards the AFM coupling (of course, provided that the orbital configuration will not change). Particularly, in order to make the bonds 1-2 and 5-6 antiferromagnetic (see Table II), the spin splitting Δ_{ex} should be reduced by about 40%. Then, if we adopt the same scaling for $J_{11'}^{\text{SE}}$ and note that $J_{11'}^{\text{DE}}$ does not depend on Δ_{ex} , the ‘screened’ NN interaction $\bar{J}_{11'}$ can be estimated as $\bar{J}_{11'} \approx J_{11'}^{\text{DE}} + \frac{5}{3}J_{11'}^{\text{SE}} = 14.2$ meV. In this case, one can also expect the formation of the helical magnetic state in the chain V1, which takes place if $\bar{J}_{11'} < -4J_{11''}$. Thus, the experimental magnetic ordering is closely related to the $\mathcal{O}1$ orbital ordering: at least on the semi-quantitative level, main details of the experimental magnetic structure are reflected in the behavior of interatomic magnetic interactions. We expect that the quantitative agreement with the experimental data could be obtained if one goes beyond the HF approximation and consider rigorously the correlation interactions. This is qualitatively consistent with calculations of the correlation energy in RPA, by starting from one-electron eigenvalues and eigenfunctions, obtained in the HF approximation. This procedure yields the following values of the total (i.e., HF plus correlation) energy differences between AFM and FM states: $\Delta E = 6$ and 2 per one formula unit for the three- and five-orbital model, respectively. Thus, already the ‘single-shot calculations’ of correlation energy substantially reduce ΔE (especially for the five-orbital model). We hope that a better agreement can be obtained by treating the correlation effects self-consistently.¹⁹

Finally, let us discuss the anisotropy of electrical resistivity. The *dc* conductivity can be evaluated using the Boltzmann's equation approach (in Rydberg atomic units):²⁰

$$\sigma_{\alpha\beta} = \frac{1}{2\pi^3} \sum_l \int_{\text{BZ}} d\mathbf{k} \tau_l(\mathbf{k}) v_l^\alpha(\mathbf{k}) v_l^\beta(\mathbf{k}) \left(-\frac{\partial f(\epsilon)}{\partial \epsilon} \right)_{\epsilon=\epsilon_l(\mathbf{k})},$$

where $\epsilon_l(\mathbf{k})$ is the band dispersion (l being the band index); $v_l^{\alpha(\beta)}(\mathbf{k}) = \partial \epsilon_l(\mathbf{k}) / \partial k_{\alpha(\beta)}$ is the group velocity; $\alpha(\beta) = x, y, \text{ or } z$ in the orthorhombic frame; $\tau_l(\mathbf{k})$ is the quasiparticle lifetime; and $f(\epsilon)$ is the Fermi distribution function. For the orthorhombic $Pnma$ symmetry, this tensor is diagonal ($\sigma_{\alpha\beta} = \sigma_{\alpha\alpha} \delta_{\alpha\beta}$), and the components of the resistivity tensor are given simply by $\rho_{\alpha\alpha} = 1/\sigma_{\alpha\alpha}$. Then, for a constant τ , one can easily evaluate the ratios $\rho_{\alpha\alpha}/\rho_{\beta\beta}$ between different components and compare it with the experimental data.

Let us start our analysis with the HM FM state. Then, for the $\mathcal{O}1$ orbital ordering, we obtain the following ratios: $\rho_{xx}/\rho_{yy} = 34$ and $\rho_{zz}/\rho_{yy} = 19$. Thus, the resistivity is highly anisotropic, where two components perpendicular to the chains $\rho_{xx} \approx \rho_{zz} \equiv \rho_{\perp}$ are about 19-34 times larger than $\rho_{yy} \equiv \rho_{\parallel}$ in the chain. Therefore, the experimentally observed anisotropy of resistivity ($\rho_{\perp}/\rho_{\parallel} > 20$, Ref. 4) can be understood already from the viewpoint of the $\mathcal{O}1$ orbital ordering, even without invoking the anisotropic $\uparrow\downarrow\uparrow\downarrow\uparrow\downarrow\uparrow$ AFM arrangement.

The orbital ordering plays a crucial role in the observed anisotropy of the resistivity tensor. For example, for the $\mathcal{O}2$ orbital ordering, the tensor $\hat{\rho} = \|\rho_{\alpha\beta}\|$ is nearly isotropic ($\rho_{xx}/\rho_{yy} \approx \rho_{zz}/\rho_{yy} \approx 1$). Similar behavior is found in the local-spin-density approximation for the HM FM state ($\rho_{xx}/\rho_{yy} = 3$ and $\rho_{zz}/\rho_{yy} = 4$).

As expected,⁴ the AFM $\uparrow\downarrow\uparrow\downarrow\uparrow\downarrow\uparrow$ spin alignment additionally enhances the anisotropy of the resistivity tensor, yielding for the $\mathcal{O}1$ orbital ordering $\rho_{xx}/\rho_{yy} = 46$ and $\rho_{zz}/\rho_{yy} = 210$. Therefore, one may ask which ordering is more important for the anisotropy of resistivity: spin or orbital one? The increase of ρ_{xx}/ρ_{yy} , in comparison with the FM alignment (for the same orbital ordering $\mathcal{O}1$), is quite modest. However, the ratio ρ_{zz}/ρ_{yy} changes by factor 10. Therefore, it is tempted to conclude that the antiferromagnetism plays at least the same role in the anisotropy of the electrical resistivity as the orbital ordering. Nevertheless, it should be also remembered that the AFM order itself is caused by the orbital order (or, at least these two orders occur concomitantly). Thus, it is probably right to say that this is the orbital ordering, which has twofold effect on the anisotropy of the electrical resistivity: direct, which is observed already in the FM state, and indirect, via formation of the anisotropic AFM structure.

IV. SUMMARY

On the basis of the first-principles electronic structure calculations, we have derived an effective low-energy model for NaV_2O_4 and employed this model for the analysis of electronic and magnetic properties of this material. The obtained transfer integrals are basically three-dimensional and by themselves do not reproduce the quasi-1D character of the electrical resistivity of NaV_2O_4 . An additional important ingredient, which yields the anisotropy of electronic and magnetic properties should be the orbital ordering, realized in the metallic state of NaV_2O_4 . We have argued that the symmetry arguments greatly simplify the analysis of the possible orbital states in NaV_2O_4 , and the proposed orbital ordering is one of the few candidates, which respects the orthorhombic $Pnma$ symmetry. The AFM spin arrangement additionally increases the anisotropy of electrical resistivity. However, the anisotropy caused by the orbital ordering is comparable with the spin contribution and is formally sufficient for reproducing the experimental value $\rho_{\perp}/\rho_{\parallel} > 20$.⁴ Moreover, the AFM spin ordering itself is driven by the orbital ordering, which increases the FM character of interactions in the chains and weakens the interactions between the chains. The sizable second-neighbor AFM interactions in the chains can be also responsible for the formation of the helical magnetic structure, which was proposed recently.⁷ Nevertheless, within the HF approximation, the FM solution was found to be slightly lower in energy than the AFM one. In order to resolve this discrepancy, we provided semi-quantitative arguments and argued that the correlation interactions, beyond the HF approximation, should probably reverse this tendency.

Acknowledgments

We would like to thank D. Hirai, T. Takayama, and H. Takagi for providing us the structure parameters of NaV_2O_4 prior to the publication.⁵ RA acknowledge the financial support from JST-PRESTO. The work of ZVP is partly supported by RFFFI-10-02-96011.

* Electronic address: pzv@ifmlrs.uran.ru

† Electronic address: SOLOVYEV.Igor@nims.go.jp

¹ C. Zener, Phys. Rev. **82** 440 (1951); P. W. Anderson and H. Hasegawa, Phys. Rev. **100** 675

- (1955); P.-G. de Gennes, Phys. Rev. **118** 141 (1960); K. Kubo and N. Ohata, J. Phys. Soc. Jpn. **33** 21 (1972).
- ² J. van den Brink and D. Khomskii, Phys. Rev. Lett. **82** 1016 (1999); I. V. Solovyev and K. Terakura, Phys. Rev. B **63** 174425 (2001).
- ³ E. Dagotto, T. Hotta, and A. Moreo, Phys. Rep. **344** 1 (2001); Y. Tokura, Rep. Prog. Phys. **69** 797 (2006).
- ⁴ K. Yamaura, M. Arai, A. Sato, A. B. Karki, D. P. Young, R. Movshovich, S. Okamoto, D. Mandrus, and E. Takayama-Muromachi, Phys. Rev. Lett. **99**, 196601 (2007); *ibid.* **101**, 129901 (2008).
- ⁵ D. Hirai, T. Takayama, A. Yamamoto, D. Hashizume, and H. Takagi (private communication).
- ⁶ H. Nozaki, J. Sugiyama, M. Månsson, M. Harada, V. Pomjakushin, V. Sikolenko, A. Cervellino, B. Roessli, and H. Sakurai, Phys. Rev. B **81**, 100410(R) (2010).
- ⁷ O. Ofer, Y. Ikedo, T. Goko, M. Månsson, J. Sugiyama, E. J. Ansaldo, J. H. Brewer, K. H. Chow, and H. Sakurai, Phys. Rev. B **82**, 094410 (2010).
- ⁸ H. Takeda, M. Itoh and H. Sakurai, J. Phys.: Conf. Ser. **273**, 012142 (2011).
- ⁹ J. Sugiyama, Y. Ikedo, T. Goko, E. J. Ansaldo, J. H. Brewer, P. L. Russo, K. H. Chow, and H. Sakurai, Phys. Rev. B **78**, 224406 (2008).
- ¹⁰ H. Sakurai, Phys. Rev. B **78**, 094410 (2008).
- ¹¹ I. V. Solovyev, J. Phys.: Condens. Matter **20**, 293201 (2008).
- ¹² Very similar parameters have been reported in Ref. 4. We have also confirmed that the use of the $T=130$ K experimental structure parameters yields essentially the same theoretical results.
- ¹³ J. Kanamori, Prog. Theor. Phys. **30**, 275 (1963).
- ¹⁴ Supplemental materials [parameters of the crystal field, transfer integrals, and matrices of Coulomb interactions].
- ¹⁵ A. I. Liechtenstein, M. I. Katsnelson, V. P. Antropov, and V. A. Gubanov, J. Magn. Magn. Matter. **67** 65 (1987).
- ¹⁶ I. V. Solovyev and K. Terakura, Phys. Rev. Lett. **82** 2959 (1999).
- ¹⁷ I. V. Solovyev and Z. V. Pchelkina, New J. Phys. **10**, 073021 (2008).
- ¹⁸ U. von Barth and L. Hedin, J. Phys. C **5**, 1629 (1972).
- ¹⁹ I. V. Solovyev, J. Phys.: Condens. Matter **23**, 326002 (2011).
- ²⁰ N. W. Ashcroft and N. D. Mermin, *Solid State Physics* (Thomson Learning, 1976).